

# An impedance probing system for real-time intraoperative brain tumour tissue discrimination

Steven S. Wong<sup>†</sup>, Jinendra Ekanayake<sup>†\*‡</sup>, Yan Liu<sup>†\*</sup>, Timothy G. Constandinou<sup>†\*</sup>

<sup>†</sup>Department of Electrical and Electronic Engineering, Imperial College London, UK

<sup>\*</sup>Centre for Bio-Inspired Technology, Institute of Biomedical Eng., Imperial College London, UK

<sup>‡</sup>Wellcome/EPSRC Centre for Interventional and Surgical Sciences, UCL, London, UK

Email: {sung.wong15, j.ekanayake, yan.liu06, t.constandinou}@imperial.ac.uk

**Abstract**—The ability to perform realtime diagnostics of tissue intraoperatively can greatly enhance the precision and effectiveness of the underlying surgery, for example, in tumour resection. To achieve this however would require a miniature tool able to perform *in situ*, *in-vivo* characterisation for distinguishing between different types of tissues. In this work, we explored the feasibility and requirements of implementing a portable impedance characterisation system for brain tumour detection. We proposed and implemented a novel system based on PCB-based instrumentation using a square four-electrode microendoscopic probe. The system uses a digital-to-analogue converter to generate a multi-tone sinusoid waveform, and a floating bi-directional voltage-to-current converter to output the differential stimulation current to one pair of electrodes. The other pair of electrodes are connected to the sensing circuit based on an instrumentation amplifier. The recorded data is pre-processed by the micro-controller and then analysed on a host computer. To evaluate the system, tetrapolar impedances have been recorded from a number of different electrode configurations to sense pre-defined resistance values. The overall system consumes 143 mA current, achieve 0.1% linearity and 15  $\mu$ V noise level, with a maximum signal bandwidth of 100 kHz. Initial experimental results on tissue were carried out on a piece of rib-eye steak. Electrical impedance maps (EIM) and contour plots were then reconstructed to represent the impedance value in different tissue region.

## I. INTRODUCTION

Surgical resection is considered as a necessary treatment for low-grade brain tumour, for high-grade tumour, precise resection should also be performed to include the most malignant tissue in the pathological specimen [1]. Complete surgical resection improves the survive rate together with chemo and radiotherapy [2], however, this requires on-site diagnostics with high precision.

Electrical stimulations are used in awake craniotomy surgery to identify the surgical margin of a brain tumour. The patient is asked to hold a conversation or perform a certain task during the surgery [3]. As the stimulation probe landed on healthy tissue, the patient will show difficulties on continuing the task. If the patient is able to continue with the tasks, this indicates the stimulation probe is located on the tumour as the tumour has no physiological functions. The neurosurgeon removes as much of the tumour as possible while avoiding the functional areas of the brain. However,

awake brain surgery is not performed in patients with obstructive sleep apnea and those who are obese. [4]

Therefore, a real-time intraoperative device detecting the surgical margin status during both resective surgery operation and biopsy procedures can greatly improve the quality of treatment by reducing excessive damage to the healthy brain tissues [5]. Ultimately reduce the mortality rate associated with brain cancer recurrence and financial burdens to the patient and healthcare providers due to cancer recurrence.

Several intraoperative methods have been used in cancer surgery, such as radio frequency-based detection (Allweis et al 2008), targeted fluorescence imaging (Van Dam et al 2011), the iKnife (Balog et al 2013, McGill et al 2013) and impedance spectroscopy based method. Among them, bioimpedance is one of the most promising physiological indicators to evaluate the physiological state of different tissue types due to the biological structure of tissues causing impedance differences. It has been reported in numerous studies [6], there are significant differences in bioimpedance of healthy and cancerous tissue in liver, prostate, breast, tongue and etc. in both in-vivo and ex-vivo measurements. [2], [7]–[10]

Through measuring the electrical properties of biological tissue of the brain tumour, there should be a difference between benign and malignant brain tissues. It is hypothesised that by observing these bioimpedance properties intraoperatively has the potential to provide clinically relevant information regarding surgical margin in a real-time manner. [11]

In this paper, we identified the essential requirements for an intraoperative impedance probing system. To prove the concept, a PCB based system was designed and implemented with an on-board current source generator and voltage amplification circuits. A tetrapolar impedance probe based on four electrodes was used and impedance across the electrode pairs are characterised via I-V measurement by using multi-tone sinusoid current waveform. Measured results were then processed by the microcontroller and host PC platform to

identify the impedance value and reconstruct the impedance map in the test samples. These results were compared with a commercial-available instruments E4980A to benchmark performance. The paper is organised as follows: Section II discusses the application requirements and introduces the system; Section III describes the circuit implementation; Section IV presents the measured results; and Section V concludes this work.

## II. SYSTEM OVERVIEW

### A. System requirement

The impedance of tissue cell is well studied for cellular processes [12] or brain tissue [13]. The impedance of normal white matter is around  $20\text{ k}\Omega$  for bovine brain [14] at DC. However, the distribution of impedance of brain tumour is not conclusive. A recent study stated the average impedance meningiomas, low-grade gliomas, and high-grade gliomas are  $530\ \Omega\text{-cm}$ ,  $160\ \Omega\text{-cm}$ , and  $498\ \Omega\text{-cm}$  respectively [13]. Therefore, the target impedance range should cover  $100\ \Omega\text{-cm}$  to  $600\ \Omega\text{-cm}$ .

The four-electrode measurement method is used due to it is not affected by polarisation as the two-electrode method. It should also be noted that due to safety concerns, the stimulation current driving the working electrodes should be smaller than  $10\ \mu\text{A}$  according to the IEC 60601-1 standard. Considering the impedance of normal and cancerous brain tissues, the voltage level received at the sensing electrodes will be in the range of  $1\ \text{mV}$  to  $6\ \text{mV}$  depending on the spacing of the electrodes.

To enable real-time intraoperative impedance characterisation, the processing time should be minimised. Therefore the MCU should be capable to convert the analogue signal if on-board ADC is used, and extract frequency domain signal by using FFT or envelop detection.

### B. System diagram

A block diagram of the system is shown in Fig. 1. It consists four parts:

- 1) A miniature probe with multi-pole electrodes to perform versatile impedance characterisation configuration.
- 2) A front-end board. It includes a voltage controlled current source to generate the stimulation source; an instrumentation amplifier to sense the voltage signal; a multiplexer array to stitching between electrodes. A standalone ADC or DAC may be added to alleviate the processing burden in the MCU.
- 3) An MCU platform to control the standalone waveform generator or ADC, and pre-process the data
- 4) A back end host computer to recon structure the data for visual display.

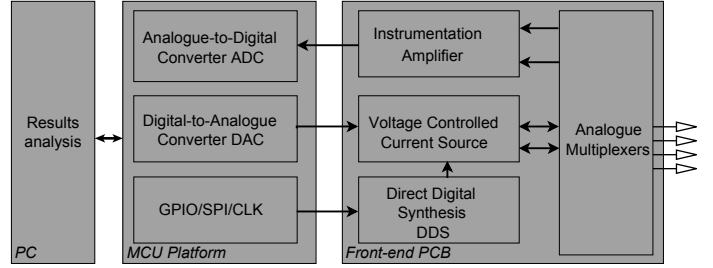


Fig. 1. System block diagram

A pre-defined stimulation waveform is stored in the MCU and sent to the DAC or the external direct digital synthesis waveform generator (DDS); the generated voltage waveform will be converted to current source with required slew rate and bandwidth. This differential current pair is directed to the target electrode pair by the multiplexers. The other pair of electrodes in the probe will sense the voltage induced by the impedance of the tissue. This voltage signal will be amplified by the instrumentation amplifier and converted into the digital domain. Then the measured waveform is processed using fast Fourier transform to obtain the impedance measurement at each frequency of interest. The impedance measurements of different connection configuration are compared with each other to identify the existence of a margin within the four electrodes and which pair of electrodes are the closest to the margin. The overall processing time is under 73 ms.

## III. CIRCUITS IMPLEMENTATION

The circuit shown in Fig. 2a uses a passive first order high-pass filter ( $R_1, C_1$ ) to remove the DC offset of the generated waveform. A buffered differential amplifier and integrator fixed the voltage across the resistor  $R_a$  regarding to the input voltage. This generates a current flowing from  $I_{op}$  to  $I_{on}$  accordingly. The return current is sunk or sourced by an opamp shown in Fig. 2b to provide a low impedance current path and allow a bias voltage to be adjusted.

Fig. 2c shows the use of instrumentation amplifier to measure the potential difference between two electrodes which is determined by the analogue multiplexer. At the same time, the analogue multiplexers define the configuration of the electrodes.

Fig. 3 shows the four tetrapolar electrode configurations constructed by the analogue multiplexers. The device measures the impedance in each configuration under a time frame of 22 ms.

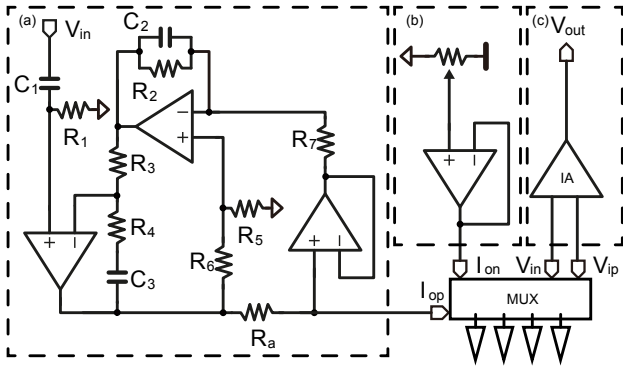


Fig. 2. Front-end analogue circuits: (a) Voltage controlled current source; (b) Voltage buffer; (c) Instrumentation amplifier

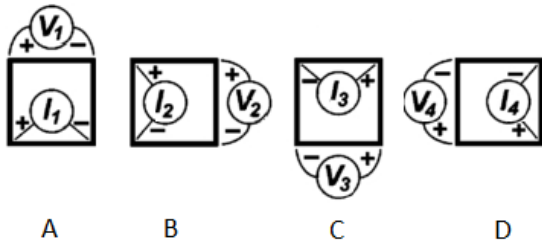


Fig. 3. Electrode configurations

#### IV. RESULTS AND DISCUSSION

##### A. Overall system and experimental setup

Fig. 4a shows the saline testing setup using the designed device with a 3-axis cramp to hold the probe over the testing area. A piece of  $1\text{ cm} \times 1\text{ cm}$  metal is placed at the centre of the glass container with 1cm deep saline solution. A 6-by-6 impedance measurements were recorded using the electrodes with a 2.54 mm spacing shown in Fig. 4b. The electrodes used are gold-plated spring loaded pins.

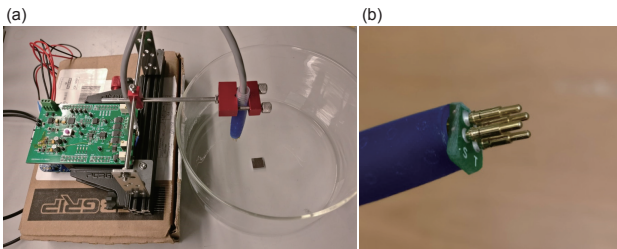


Fig. 4. (a) Overview of the implemented system for saline testing setup; (b) The probe with four-electrodes configuration.

##### B. Electrical verification

Fig. 5a and b show the recorded DAC output and the signal at the ADC input respectively. It can be observed from the ADC input, the effect of polarisation caused by a build up of charge occurred on the electrodes in the presence of water molecules and hydrogen ions. The insertion of electrodes causes the release of electrolytes from the surrounding and results in a poorly conductive area on the electrodes. Hence,

the decaying voltage can be observed from Fig. 5b including the contribution from the saline solution being a capacitive load.

Fig. 5c and d show the measured signal and the corresponding fast Fourier transform (FFT) output. The capacitive effect introduced a negative offset at the instrumentation amplifier inputs, and the sampled waveform is invalid as the ADC is unable to measure signal beyond the ground (0V). The noise shown in the FFT results is caused by missing negative voltages.

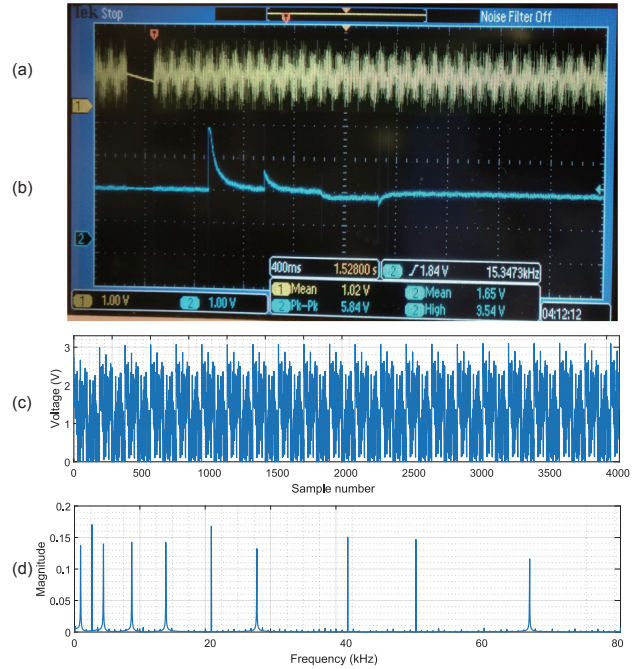


Fig. 5. Measured waveform from DAC output and working electrodes

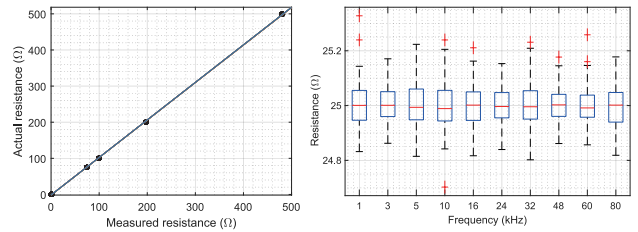


Fig. 6. Measured waveform from DAC output and working electrodes

The implemented device was calibrated with a  $25\ \Omega$  resistor with 0.5% tolerance, the typical error of the device is below 2% with a resolution of  $1\ \Omega$ . Measurements on different resistor values have shown the device has a linearity of 0.1%. And the error increases as the tissue impedance decreases, as the measured noise level approaches the thermal noise floor.

##### C. Biological tissue measurement

The high impedance area represents the fat on the steak. The contour plot is able to illustrate the margin of the fat and

muscle fibre with the light blue colour region.

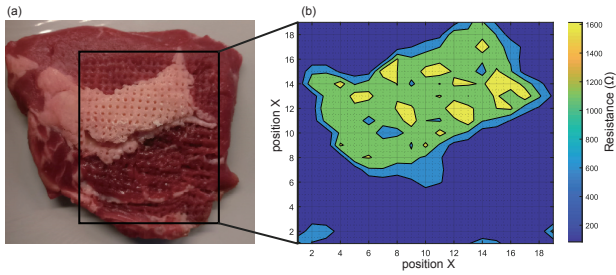


Fig. 7. a) The biological sample, a piece of steak; b) reconstructed resistance mapping using the implemented device.

## V. CONCLUSION

In this work, a bioimpedance spectroscopy device was implemented to perform real-time tissue analysis. By using a multi-tone sinusoid waveform, the implemented system is capable to perform impedance characterisation from 1 kHz to 80 kHz with a minimum resolution of  $1 \Omega$ . The fabricated system was verified in an electronic dummy model, saline solution and biological sample, a piece of rib-eye steak under controlled temperature condition. The measured results demonstrated that the instrument has achieved a maximum 2% error, a linearity of 0.1% and a power consumption of 736.7 mW.

The designed instrument was compared with measurement results using the Agilent E4980A Precision LCR meter, the implemented system had achieved similar performance in terms of relative impedance and had reaffirmed the feasibility of the technique. As proof of concept, it has been shown that the design is versatile to different bioimpedance. With adjustable gain and configurable waveform, it can be used on various tissues and conductive solutions with various impedance range.

## REFERENCES

- [1] L. M. DeAngelis, "Brain tumors," *New England Journal of Medicine*, vol. 344, no. 2, pp. 114–123, 2001.
- [2] A. Pathiraja *et al.*, "Detecting colorectal cancer using electrical impedance spectroscopy: an ex vivo feasibility study," *Physiological measurement*, vol. 38, no. 6, p. 1278, 2017.
- [3] S. Kieffer, "Awake brain surgery (intraoperative brain mapping) — imaging services — johns hopkins intraoperative neurophysiological monitoring unit (ionm)." [Online]: [https://www.hopkinsmedicine.org/neurology\\_neurosurgery/centers\\_clinics/ionm/types/intraoperative-brain-mapping.html](https://www.hopkinsmedicine.org/neurology_neurosurgery/centers_clinics/ionm/types/intraoperative-brain-mapping.html)
- [4] K. Candiotti, S. Sharma, and R. Shankar, "Obesity, obstructive sleep apnoea, and diabetes mellitus: anaesthetic implications," *BJA: British Journal of Anaesthesia*, vol. 103, pp. i23–i30, 12 2009. [Online]: <https://doi.org/10.1093/bja/aep294>
- [5] S. Khan *et al.*, "Towards intraoperative surgical margin assessment and visualization using bioimpedance properties of the tissue," in *Medical Imaging: Computer-Aided Diagnosis*, 2015.
- [6] T. Morimoto *et al.*, "A study of the electrical bio-impedance of tumors," *Investigative Surgery*, vol. 6, no. 1, pp. 25–32, 1993. [Online]: <https://www.ncbi.nlm.nih.gov/pubmed/8452822>
- [7] T. J. C. Faes, H. A. van der Meij, J. C. de Munck, and R. M. Heethaar, "The electric resistivity of human tissues (100Hz-10MHz): a meta-analysis of review studies," *Physiological Measurement*, vol. 20, no. 4, pp. R1–R10, nov 1999. [Online]: <https://doi.org/10.1088/0967-3334/20/4/R1>
- [8] N. Chauveau *et al.*, "Ex vivo discrimination between normal and pathological tissues in human breast surgical biopsies using bioimpedance spectroscopy," *Annals of the New York Academy of Sciences*, vol. 873, pp. 42–50, Apr 20, 1999.
- [9] A. Pathiraja *et al.*, "Detecting colorectal cancer using electrical impedance spectroscopy: an ex vivo feasibility study," *Physiological measurement*, vol. 38, no. 6, p. 1278, Jun 2017. [Online]: <https://www.ncbi.nlm.nih.gov/pubmed/28333038>
- [10] S. Laufer *et al.*, "Electrical impedance characterization of normal and cancerous human hepatic tissue," *Physiological Measurement*, vol. 31, no. 7, pp. 995–1009, Jul 1, 2010. [Online]: <http://iopscience.iop.org/0967-3334/31/7/009>
- [11] S. Hu *et al.*, "Realtime imaging of brain tumor for imageguided surgery," *Advanced Healthcare Materials*, vol. 7, no. 16, p. n/a, Aug 22, 2018. [Online]: <https://onlinelibrary.wiley.com/doi/abs/10.1002/adhm.201800066>
- [12] W. Wang *et al.*, "Single cells and intracellular processes studied by a plasmonic-based electrochemical impedance microscopy," *Nature chemistry*, vol. 3, no. 3, p. 249, 2011.
- [13] J. Latikka and H. Eskola, "The resistivity of human brain tumours in vivo," *Annals of Biomedical Engineering*, vol. 47, no. 3, pp. 706–713, Mar 2019. [Online]: <https://doi.org/10.1007/s10439-018-02189-7>
- [14] T. Parupudi, A. L. Garner, and R. S. P. University, "Electrical impedance measurement as biomarker for brain tumors," in *2018 Electrostatics Joint Conference*, 2018.